ed, but it is equivocal (12). The 1968 Borrego Mountain earthquake shows a pattern similar to that of the Landers event: The rupture appeared to hesitate at a dilatational stepover, where surface slip was a minimum (13), but geodetic surveys show no clear minimum in slip at depth at the stepover (14).

Our observations of fault zone–guided waves are consistent with some aspects of existing fault-zone rupture models. The separation of simple crack by a barrier is a feature of the specific barrier model (15). For an M7.4 event, this model predicts that cracks have a diameter of 15 km, close to the dimension of the waveguides that we observed. Other models describe alternation between rupture near the Rayleigh velocity and slower rupture propagation (16).

We interpret the Landers rupture as a combination of rapid rupture on planar fault surfaces and hesitation at fault surface complexity. The rupture history is a function of fault geometry rather than available strain energy. Hesitancy is an important determinant of rupture energetic and strong motion. The ability to use guided waves to locate the fault plane precisely furthers an understanding of the rupture process (17).

It is not clear whether the fault zone waveguide originated primarily during the recent Landers earthquake or whether it represents a wear zone that has accumulated over geological time. In the former view, which has its roots in fracture mechanics, the waveguide may represent the width of the process zone, a zone of inelastic deformation around the propagating crack tip.

Theoretical work or fault mechanics suggests that $P/L$ is of order $10^{-2}$, where $P$ is the dynamic process zone width and $L$ is the rupture length (18). If we take $L = 30$ km, the length of the two main subfaults, $P$ is 300 m, which is consistent with our observations of the width of the fault zone waveguide. This value is not conclusive as to the origin of the waveguide, however, because the same scaling arguments yield a total fault displacement, $d$, of 200 m to 2 km, which is a reasonable value for the recent net offset of the faults. Our data do not indicate that the fault zone has widened with depth. The 200-m width of the waveguide is consistent with the theoretical modeling of other seismic parameters (19). Because the waveguide disrupted at the fault bend and the rupture hesitated at the bend, which would tend to reduce $P$, we tentatively conclude that the waveguide is the result of dynamic rupture during the Landers event.

## REFERENCES AND NOTES

1. C. H. Scholz, *The Mechanics of Earthquakes and Faulting* (Cambridge Univ. Press, New York, 1990); W. D. Mooney and A. Ginzburg, *Pure Appl. Geophys.* **124**, 141 (1986).
2. V. F. Cormier and P. Spudich, *Geophys. J. R. Astron. Soc.* **79**, 411 (1984); Y.-G. Li, P. Leary, K. Aki, P. Malin, *Science* **249**, 763 (1990); Y.-G. Li and P. C. Leary, *Bull. Seismol. Soc. Am.* **80**, 1245 (1990); A. Michelini and T. V. McEvilly, *ibid.* **81**, 524 (1991).
3. Y.-G. Li, K. Aki, D. Adams, A. Hasemi, W. H. K. Lee, *J. Geophys. Res.* **99**, 11705 (1994).
4. W. H. K. Lee, Y.-G. Li, R. Banfill, D. A. Dodge, *U.S. Geol. Surv. Open-File Rep.*, in press.
5. A joint field experiment between the Southern California Earthquake Center and the U.S. Geological Survey at Menlo Park.
6. P. C. Leary, Y.-G. Li, K. Aki, *Geophys. J. R. Astron. Soc.* **91**, 461 (1987); Y.-G. Li, P. C. Leary, K. Aki, *ibid.*, p. 485.
7. D. J. Wald and T. H. Heaton, *Bull. Seismol. Soc. Am.* **84**, 668 (1994).
8. B. P. Cohee and G. C. Beroza, *ibid.*, p. 692.
9. A. M. Johnson, R. W. Fleming, K. M. Cruikshank, *ibid.*, p. 499.
10. K. Sieh *et al.*, *Science* **260**, 171 (1993).
11. S. L. Beck and L. J. Ruff, *J. Geophys. Res.* **90**, 6773 (1985); T. M. Boyd and J. L. Nabelek, *Bull. Seismol. Soc. Am.* **78**, 1653 (1988); H. Houston and E. R. Engdahl, *Geophys. Res. Lett.* **16**, 1421 (1989); L. Dorbath *et al.*, *Geophys. J. Inter.* **108**, 309 (1992); M. Kikuchi, H. Kanamori, K. Satake, *J. Geophys. Res.* **98**, 15797 (1993); C. J. Ammon, T. Lay, A. A. Velasco, J. E. Vidale, *Bull. Seismol. Soc. Am.*, in press.
12. W. H. Bakun *et al.*, *Science* **225**, 288 (1984); G. C. Beroza and P. Spudich, *J. Geophys. Res.* **93**, 6275 (1988); A. J. Michael, *Bull. Seismol. Soc. Am.* **78**, 1199 (1988).
13. R. H. Sibson, *Philos. Trans. R. Soc. London* **317**, 63 (1986).
14. W. Thacher and M. G. Bonilla, in *Fault Segmentation and Controls of Rupture Initiation and Termination*, D. P. Schwartz and R. H. Sibsons, Eds. (U.S. Geological Survey, Palm Springs, CA, 1988), vol. 89-315, p. 386.
15. A. S. Papageorgiou and K. Aki, *Bull. Seismol. Soc. Am.* **73**, 953 (1983); K. Aki, *Tectonophysics* **211**, 1 (1992).
16. J. Boatwright, *Bull. Seismol. Soc. Am.* **72**, 1049 (1982); *ibid.* **78**, 489 (1988).
17. R. A. Harris and S. M. Day, *J. Geophys. Res.* **98**, 4461 (1993); E. Fukuyama and T. Mikumo, *ibid.*, p. 6529; H. Quin, *Tectonophysics* **175**, 93 (1990); K. Aki, in (*14*), pp. 1–9; C. H. Scholz, *Geology* **15**, 493 (1987).
18. C. H. Scholz, N. H. Dawers, J.-Z. Yu, M. H. Anders, P. A. Cowei, *J. Geophys. Res.* **98**, 21951 (1993).
19. Y. Ida, *Bull. Seismol. Soc. Am.* **63**, 959 (1973); K. Aki, *J. Geophys. Res.* **92**, 1349 (1987); C. Marone and B. Koyanagi, *Nature* **362**, 618 (1993).
20. E. Haukksson, L. M. Jones, K. Hutton, D. Eberhart-Phillips, *J. Geophys. Res.* **98**, 19835 (1993).
21. J. E. Vidale, *Bull. Seismol. Soc. Am.* **80**, 493 (1990).
22. We thank R. White, D. Harlow, S. Maichnick, and R. Banfill for helping to deploy the seismometers; G. Beroza, J. Boatwright, and W. Mooney for providing insight into fault zone structure; H. Houston and C. Sammis for improving the manuscript; E. Haukkson for providing unpublished relocations of Landers aftershocks; and K. M. Cruikshank and an anonymous reviewer for useful comments and suggestions. Supported by the Southern California Earthquake Center under National Science Foundation grant EAR-8920136 and U.S. Geological Survey grant 14-0A-0001-A0899.

5 April 1994; accepted 31 May 1994

---

# Stepwise Formation of Multilayered Nanostructural Films from Macromolecular Precursors

Elaine R. Kleinfeld and Gregory S. Ferguson*

**Sequential adsorption of a cationic polyelectrolyte and individual sheets of the silicate mineral hectorite has allowed controlled, stepwise formation of multilayered films on silicon wafers. Each component adsorbs rapidly by an ion-exchange mechanism, and x-ray diffractometry indicates structural order even in films with thicknesses greater than 0.2 micrometer. The large lateral extent of the silicate sheets (about 25 to 35 nanometers) allows each layer to cover any packing defects in the underlying layer, thus preserving structural order in the growing film. With careful choice of component materials, this method should allow for the preparation of multilayered films with a variety of technologically important properties.**

Ultrathin films and multilayered structures are important for many applications, including x-ray optics (1), nonlinear optics (2), and microelectronics (3, 4), and are under investigation for use as chemical sensors (5). Langmuir-Blodgett (LB) deposition (6–8) of preformed monolayers from a gas-liquid interface to a solid planar substrate can provide well-ordered, densely packed mono- and multilayered systems useful for these applications. Unfortunately, LB multilayers are mechanically unstable, held together primarily by van der Waals forces (7, 8). Spontaneous self-assembly (SA) of molecular adsorbates onto solid substrates (7) can also provide densely packed monolayers and has recently been extended to the formation of multilayers in selected systems (5, 9, 10). The presence of covalent bonds or ionic attraction between layers provides additional stability not seen in LB systems; however, in many SA systems, adsorption of multilayers displaying structural order has proven difficult. In this report, we describe a method for the stepwise preparation of ordered multilayered films from ultrathin ($\sim$1 nm) layers of organic and inorganic macromolecules.

---

Department of Chemistry, Lehigh University, Bethlehem, PA 18015, USA.

*To whom correspondence should be addressed.

Films with thicknesses greater than 0.2 μm have been prepared that have sufficient structural order to diffract x-rays.

Our approach involves sequential adsorption of the polyelectrolyte polydiallyldimethylammonium chloride (PDDA) (1)

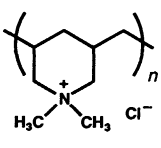

1

and exfoliated sheets of synthetic hectorite, a mica-type layered silicate [Laponite RD (*11*)]. When stirred in water, this silicate mineral exfoliates into crystalline, quasi–two-dimensional sheets that are 0.96 nm thick and about 25 to 35 nm in diameter. The sheets bear a negative charge, which is balanced in the precursor by interlamellar sodium cations that can undergo ion exchange reactions with other cationic materials (*12–14*). Our choice of PDDA for this study reflects the strong affinity of hectorite and related minerals for tetraalkylammonium compounds (*15*).

To prepare a substrate for a multilayered structure, a (100)-oriented single-crystal silicon wafer bearing a native oxide was cut into small pieces (~1 cm by 2 cm) and then cleaned to provide a hydroxylated surface (*16*). A 5% (w/w) aqueous solution of PDDA was dripped onto this substrate, and after ~5 s, it was rinsed with water and blown dry with nitrogen. Subsequently, a 0.2% (w/w) aqueous dispersion of hectorite was dripped onto the surface, and after ~5 s, it was rinsed with water and blown dry with nitrogen. By repetition of this simple two-step adsorption cycle (Scheme 1), films thicker than 0.2 μm could be prepared in less than 2 hours. An x-ray photoelectron survey spectrum of a silicon substrate that had been treated with PDDA, then hectorite, and then PDDA confirmed the presence of those elments in the silicate and the polymer: Si, O, Mg, C, N, and Cl (*11*). The absence of sodium, which is present in the precursor mineral as an interlamellar counterion, indicates that it had been exchanged for the cationic polymer. The low expected concentration of lithium on the surface and the low sensitivity factor of the Li 1*s* orbital explain the absence of this peak (*17*).

Optical ellipsometry was used to monitor the growth in thickness of the multilayer structures. In a typical cycle, ~1.1 nm of polymer and ~2.1 nm of silicate were adsorbed (Fig. 1A). The ellipsometry indicated a linear increase in the thickness of the structures with the number of adsorption cycles (Fig. 1B) (*18*). The average thickness added per adsorption cycle increased slightly as the number of cycles increased, from ~3.2 nm after five cycles to ~3.6 nm after 60 cycles. The thickness of the multilayer samples was remarkably even: Ellipsometric measurements taken on any single hectorite-terminated sample typically agreed to within ±2%, and the majority of samples showed less than one-half of that variability. Sample-to-sample reproducibility was also very good. Three samples prepared on different days with 22 cycles had average thicknesses within 2% of one another. If the adsorption times were doubled, to 10 s, the average amount of each component that was adsorbed onto the sample surface varied by ~0.1 nm or less, which is within experimental error. If adsorptions were allowed to proceed for extended times (15 min), however, the average thickness added in each of the first five cycles increased from ~3.2 to ~3.8 nm.

As an increasing number of layers was adsorbed, samples progressed through a series of well-defined colors because of interference effects, as has also been noted for LB (6, 8) and SA (9) multilayered systems. No cloudiness was observed in the samples, and the colors were uniform, with only a small region (less than 1 mm wide) at the sample edges showing nonuniformity.

At the outset of this work, we expected the hectorite to be adsorbed onto the sample surface in a controlled manner by ion exchange of the ammonium groups of the surface-bound polymer for the alkali metal counterions of the anionic hectorite sheets. Once the surface was covered with a layer of hectorite, further adsorption of the silicate should be inhibited by coulombic repulsion between the anionic sheets. The adsorption of approximately two hectorite layers (2.0 to 2.2 nm) per adsorption cycle indicates that some of the polymer is associated sufficiently loosely with the surface that it is displaced in the subsequent hectorite adsorption and becomes the "glue" for addition of a second layer of hectorite (Scheme 1). Consistent with this proposed mechanism, the amount of hectorite adsorbed in a particular cycle could be controlled by varying the amount of polymer adsorbed in that cycle (*19*). Furthermore, only a single layer of hectorite was adsorbed onto a single layer of a monomeric ammonium salt that was covalently bound to the silicon substrate (*20*). Ion exchange has been used for the adsorption of composite films (*21*), but the combination of structural order and 1- to 2-nm lattice spacings that characterize PDDA-hectorite multilayers has not been seen previously.

Because the hectorite sheets in a single adsorbed layer will have packing imperfections (that is, open space at their boundaries), the linearity of multilayer growth (Fig. 1B) indicates that this system is self-healing with respect to addition of subsequent layers. We infer that the large lateral

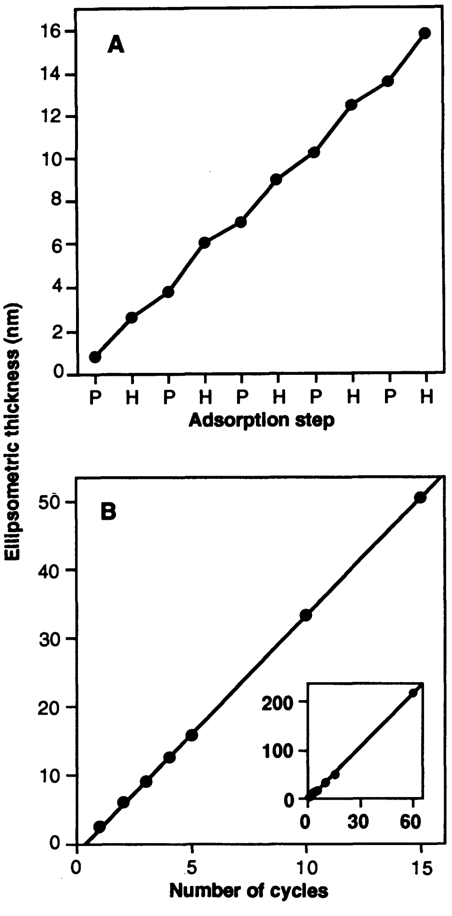

**Fig. 1.** Ellipsometric thickness of a multilayered structure on a single-crystal silicon substrate as a function of the number of adsorption cycles for (**A**) individual steps in five cycles (P, polymer; H, hectorite) and (**B**) 15 and (**inset**) 60 complete PDDA-hectorite cycles. Lines shown in (B) are best fits to the data. The native oxide on silicon is not included in the reported thicknesses.

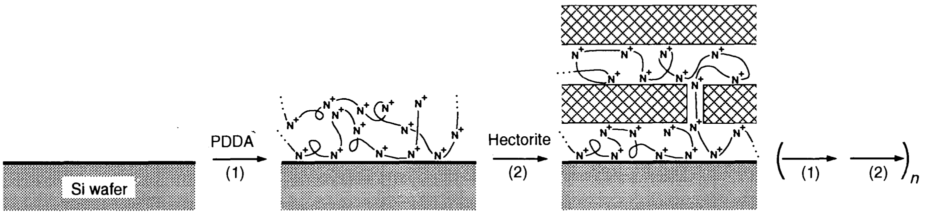

**Scheme 1.**

extent of the sheets allows coverage of regions where the underlying layer is incomplete. In contrast, other multilayer preparations that rely on the formation of each layer through reaction of individual adsorbed molecules with molecules from the contacting solution are less able to recover lost order; in such systems, defects may occur to create unreactive patches that do not participate further in multilayer growth, resulting in a decay in structural order as an increasing number of layers is added (*9, 22*).

The x-ray diffraction (XRD) data provided additional evidence for the presence of structural order in PDDA-hectorite multilayered films (*23*). A grazing-incidence XRD pattern of a multilayer formed by 60 adsorption cycles is shown in Fig. 2. The peak at $2\theta = 6.1°$, a (001) reflection, corresponds to a layer spacing of 1.45 ± 0.03 nm; (003), (004), and (005) reflections, found at 18.4°, 25.1°, and 30.8°, respectively, indicate layer spacings of 1.44 ± 0.02, 1.42 ± 0.02, and 1.45 ± 0.03 nm (*24*). These spacings are consistent with an ABABAB alternation of the silicate sheets (0.96 nm thick) with polymer layers that are ~0.4 to 0.5 nm thick. We expect that the silicate lattices in adjacent layers lack registry (*25*), causing an increase in the breadth of the $(00\ell)$ peaks (*26*). Because of this extraneous source of broadening, application of the Scherrer equation (*27*) to the (001) reflection (full width at half height, 1.6°) can only provide a lower limit (5.1 nm) to the size of ordered domains in the direction normal to the substrate surface (*26*). Additional peaks in the XRD pattern can be attributed to the substrate because they also occurred in diffractograms of bare silicon wafers (*28*). The absence of reflections corresponding to the hectorite starting material indicates that no intact three-dimensional crystallites of the precursor have been incorporated into the structure, and the absence is also consistent with the sheets being preferentially oriented parallel or near parallel to the substrate surface (*29*). The tendency of exfoliated silicate sheets to restack in a parallel arrangement has been well established (*14, 25*).

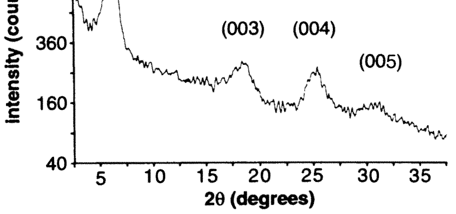

**Fig. 2.** The x-ray diffractogram of a sample that had been treated with 60 adsorption cycles (*28*). The basal reflections indicate a lattice spacing of ~1.4 nm.

Atomic force microscopy (AFM) was used to examine the surface topography of the multilayered samples. An image of a 2 µm by 2 µm area on a sample that had been treated with one PDDA-hectorite adsorption cycle (Fig. 3A) (*30*), obtained in attractive (noncontact) mode, reveals the individual hectorite sheets adsorbed at the sample surface. A sample that had been treated with five adsorption cycles gave a similar AFM image, and an image of a clean wafer was nearly flat. A representative trace across the surface (Fig. 3B) gives an idea of the lateral dimension of individual platelets and the roughness of the surface.

The preparative method described here offers a potentially powerful strategy for building ordered organic-inorganic thin films with systematic control over both structure and thickness. It should be readily adaptable to other systems that incorporate other substrates, included molecules, and inorganic sheets (*31*). The use of gold substrates, for example, coated with an ω-mercaptoalkylammonium compound to promote adsorption of the first silicate layer, should allow electrodes to be prepared with complex but controllable barrier layers and allow evaluation of the performance of these multilayered structures as electrical insulators (*4, 32*), diffusional barriers (*13*), or mediators for electron transfer (*33*). Deposition of crystalline materials onto sheet silicates, including oxides (*34*) and metals (*35*), has been demonstrated, indicating that our multilayer films may be of interest as substrates for growth of other materials. Metal-terminated structures, for example, may be of particular interest as metal-insulator-semiconductor (MIS) or metal-insulator-metal (MIM) devices (*4*). Preparation of multilayer assemblies with nonlinear optical activity (*2, 36*) may be possible if polar molecules (monomeric or polymeric) can be oriented noncentrosymmetrically between inorganic sheets. Finally, adaptation of this method to other layered materials with known intercalation chemistry, including metal dichalcogenides (*29*), metal halides (*37*), and layered metal oxides such as $V_2O_5$ (*38*) and FeOCl (*39*), may allow stepwise preparation of multilayered structures with a range of electronic band gaps.

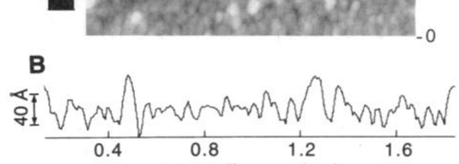

**Fig. 3.** (**A**) An AFM image, obtained in attractive mode, of a sample that had been treated with one adsorption cycle. The image has been flattened. (**B**) Trace taken horizontally, about one-fourth of the way up from the bottom of the image shown in (A).

## REFERENCES AND NOTES

1. T. W. Barbee Jr., *Proc. Soc. Photo-Opt. Instrum. Eng.* **563**, 2 (1985); E. Spiller, in *Physics, Fabrication, and Application of Multilayered Structures*, P. Dhez and C. Weisbuch, Eds. (Plenum, New York, 1988), pp. 271–309.
2. H. E. Katz *et al.*, *Science* **254**, 1485 (1991).
3. H. E. Katz and M. L. Schilling, *Chem. Mater.* **5**, 1162 (1993).
4. L. J. Kepley, D. D. Sackett, C. M. Bell, T. E. Mallouk, *Thin Solid Films* **208**, 132 (1992).
5. G. Cao, H.-G. Hong, T. E. Mallouk, *Acc. Chem. Res.* **25**, 420 (1992).
6. K. B. Blodgett, *J. Am. Chem. Soc.* **57**, 1007 (1935).
7. A. Ulman, *An Introduction to Ultrathin Organic Films: From Langmuir-Blodgett to Self-Assembly* (Academic Press, Boston, MA, 1991).
8. G. L. Gaines Jr., *Insoluble Monolayers at Liquid-Gas Interfaces* (Interscience, New York, 1966).
9. N. Tillman, A. Ulman, T. L. Penner, *Langmuir* **5**, 101 (1989).
10. H. Lee, L. J. Kepley, H.-G. Hong, T. E. Mallouk, *J. Am. Chem. Soc.* **110**, 618 (1988); S. D. Evans, A. Ulman, K. E. Goppert-Berarducci, L. J. Gerenser, *ibid.* **113**, 5866 (1991).
11. Laponite RD (synthetic hectorite, Laporte Industries, Luton, UK) was reported to have an elemental composition consistent with the approximate molecular formula $Si_8[Mg_{5.5}Li_{0.4}H_{4.0}O_{24.0}]^{0.7-}Na_{0.7}{}^{0.7+}$. See J. D. F. Ramsay, *J. Colloid Interface Sci.* **109**, 441 (1986).
12. M. S. Dresselhaus, Ed., *Intercalation in Layered Materials* (Plenum, New York, 1986).
13. K. Yano, A. Usuki, A. Okada, T. Kurauchi, O. Kamigaito, *J. Polym. Sci. A Polym. Chem.* **31**, 2493 (1993).
14. J. W. Jordan, *J. Phys. Colloid Chem.* **53**, 294 (1949).
15. B. Brahimi, P. Labbe, G. Reverdy, *Langmuir* **8**, 1908 (1992).
16. Silicon substrates were cleaned with a 2:1 (v/v) solution of concentrated $H_2SO_4$ and 30% $H_2O_2$ (caution: this solution reacts violently with organic materials) and were thoroughly rinsed with purified water.
17. The survey spectrum was obtained on a Scienta (Uppsala, Sweden) ESCA-300 spectrometer with Al Kα radiation. In addition to the elements named, this spectrum revealed a trace amount of oxidized sulfur on the sample (S 2*s*, 232.0 eV), most likely a result of the cleaning procedure used [W. Kern, *J. Electrochem. Soc.* **137**, 1887 (1990)].
18. All data in Fig. 1 are averages over three points on each of two samples treated side-by-side, with the exception of the point at 60 cycles, which is an average over five points on one sample. Similar thicknesses were seen on other samples. More extensive rinsing during the preparation led to

adsorption of slightly less material per cycle (by ~2 Å). The refractive index assumed, 1.5, was representative of the values measured ellipsometrically (1.48 to 1.59) on structures greater than 50 nm in thickness. The measured refractive index increased with increasing multilayer thickness.
19. The concentration of the polymer solution was diluted in increments from 20 to 0.05% (w/w), and in response, the amount of polymer adsorbed per cycle decreased monotonically from 2.1 to 0.1 nm. The amount of hectorite adsorbed per cycle correspondingly fell monotonically from 2.7 to 0.6 nm.
20. Adsorption of $(CH_3O)_3Si(CH_2)_3N(CH_3)_3Cl$ onto a silicon wafer from a chloroform solution gave a covalently bound layer with an ellipsometric thickness of ~6 Å.
21. G. Decher *et al.*, *Polym. Prepr.* **34**, 745 (March 1993); Y. Lvov, H. Haas, G. Decher, H. Möhwald, A. Kalachev, *J. Phys. Chem.* **97**, 12835 (1993); R. K. Iler, *J. Colloid Interface Sci.* **21**, 569 (1966).
22. H. Byrd *et al.*, *J. Am. Chem. Soc.* **116**, 295 (1994).
23. Data were obtained on a Philips APD 3720 powder x-ray diffractometer with Cu Kα radiation.
24. The average growth in thickness per cycle as determined by ellipsometry was not an even multiple of the 1.4-nm periodicity revealed by XRD. This result reflects the fact that ellipsometry gives the average thickness within an illuminated spot (~1 mm$^2$ in area). A measured increase in thickness of 3.6 nm may indicate that in any one cycle, some regions within the illuminated spot gained two layers, while others gained three.
25. H. S. Peiser *et al.*; Eds., *X-Ray Diffraction by Polycrystalline Materials* (Wright, Bristol, UK, 1955), p. 466.
26. V. A. Drits and C. Tchoubar, *X-Ray Diffraction by Disordered Lamellar Structures* (Springer-Verlag, New York, 1990), pp. 21–22.
27. B. E. Warren, *X-Ray Diffraction* (Addison-Wesley, Reading, MA, 1969), pp. 251–254.
28. The XRD data presented in the original manuscript of this report had two additional features: a very sharp peak at 33.0° (*d* = 0.27 nm), and a broad, very low intensity peak at ~13.3° (*d* = 0.66 nm). Both of these features were absent if samples were rinsed more extensively both during multilayer formation and shortly before XRD analysis. The full width at half height of the (001) peak in that pattern was 2.0°, indicating a domain size of 3.6 nm.
29. W. M. R. Divigalpitiya, R. F. Frindt, S. R. Morrison, *Science* **246**, 369 (1989).
30. The AFM image was acquired with a Parks Scientific Instruments Autoprobe cp with an Ultralever (silicon) probe tip.
31. We have recently formed PDDA-hectorite multilayers on gold and on copper and have formed multilayered structures on silicon using a different polyelectrolyte, poly(*N*-methyl-4-vinylpyridinium bromide).
32. M. D. Porter, T. B. Bright, D. L. Allara, C. E. D. Chidsey, *J. Am. Chem. Soc.* **109**, 3559 (1987).
33. H. Lee, L. J. Kepley, H.-G. Hong, S. Akhter, T. E. Mallouk, *J. Phys. Chem.* **92**, 2597 (1988).
34. S. Steinberg *et al.*, *Science* **260**, 656 (1993).
35. H.-Y. Liu, F.-R. F. Fan, A. J. Bard, *J. Electrochem. Soc.* **132**, 2666 (1985); M. H. B. Stiddard, *Thin Solid Films* **94**, 1 (1982); R. Waser and K. G. Weil, *J. Electroanal. Chem.* **150**, 89 (1983); A. Putnam, B. L. Blackford, M. H. Jericho, M. O. Watanabe, *Surf. Sci.* **217**, 276 (1989).
36. D. Li *et al.*, *J. Am. Chem. Soc.* **112**, 7389 (1990).
37. P. Day and R. D. Ledsham, *Mol. Cryst. Liq. Cryst.* **86**, 163 (1982).
38. C.-G. Wu, M. G. Kanatzidis, H. O. Marcy, D. C. DeGroot, C. R. Kannewurf, in *Lower-Dimensional Systems and Molecular Electronics*, R. M. Metzger, P. Day, G. C. Papavassiliou, Eds. (Plenum, New York, 1991), pp. 427–433.
39. J. F. Bringley and B. A. Averill, *Chem. Mater.* **2**, 180 (1990).
40. We gratefully acknowledge O. Shaffer for assistance in obtaining AFM images, D. Simpson for helpful discussions regarding the interpretation of x-ray diffractograms (obtained with the assistance of G. Yasko), A. Miller and D. Carey for technical assistance with the x-ray photoemission spectroscopic analysis, and Lehigh University for supporting the Scienta ESCA-300 Laboratory. Silicon wafers used as substrates were donated by WaferNet. The synthetic hectorite was donated by Laporte Industries to D. Hseih, who kindly provided us with a sample. E.R.K. gratefully acknowledges financial support from AT&T Bell Laboratories in the form of a Ph.D. Scholarship.

16 February 1994; accepted 16 May 1994

---

# Size Dependence of a First Order Solid-Solid Phase Transition: The Wurtzite to Rock Salt Transformation in CdSe Nanocrystals

S. H. Tolbert and A. P. Alivisatos

**Measurements of the size dependence of a solid-solid phase transition are presented. High-pressure x-ray diffraction and optical absorption are used to study the wurtzite to rock salt structural transformation in CdSe nanocrystals. These experiments show that both the thermodynamics and kinetics of this transformation are altered in finite size, as compared to bulk CdSe. An explanation of these results in the context of transformations in bulk systems is presented. Insight into the kinetics of transformations in both bulk and nanocrystal systems can be gained.**

Studies of phase transitions in condensed phases have generally assumed that pressure, temperature, and composition are the only variables of importance in determining stable states of materials. The reduction of melting temperature in finite size clusters (*1*, *2*), however, has proven that the physical extent of a material can also be an important variable in determining transition points. Recently, studies of clusters in both the gas and condensed phases have led to numerous instances in which one bonding geometry appears to be favored over others in finite size, as compared to the bulk (*3*). To help understand these observations, we investigated the relative stability of two different solid bonding geometries in clusters as a function of the size. Our goal was to force a nanocrystal system between two solid structures and measure the energy difference between them. We achieved this goal through the application of very high pressures.

This study of the size dependence of a solid-solid phase transition also reveals important dynamical effects that are not observed in size-dependent melting. In a bulk system, the thermodynamic definition of a phase transition is the point where the fluctuation length scale diverges. In a nanocrystal, this length scale is intrinsically limited by the size of the crystallite. Additionally, in most inorganic solid-solid transitions, there is a substantial barrier to transition at room temperature. As a consequence, the bulk solid converts at a pressure well above its thermodynamic transition pressure. This barrier is usually related to the fragmentation of bulk materials into finite domains upon transition. Because nanocrystals are substantially smaller than these domains, it is likely that the barriers to transition will be altered at finite sizes. By studying structural transformations in nanocrystals, we can learn about the nature of the barrier and the dynamics of the transition in bulk as well as in nanocrystals.

While understanding the altered stability in finite size is of fundamental interest, it also has practical implications in a variety of fields ranging from microelectronics and materials science to geophysics. Variation in stability with size could provide the materials scientist with a method for control of the properties of materials. By using nanocrystals whose surface can be deliberately altered, one may be able to vary the phase diagram at will. In geophysics as well, the notion of a domain size dependence of high-pressure and high-temperature phase transitions could affect our understanding of stable states.

The system that we have chosen for these experiments is CdSe semiconductor nanocrystals. Recent developments in synthetic methods make this a particularly well controlled and characterized test system. Nearly monodisperse, spherical nanocrystals ranging in radius from 10 to 30 Å can now be produced (*4*, *5*). Unlike the many nanocrystalline materials that appear to be amorphous, these nanocrystals have a wurtzite structure and are highly crystalline, with less than one fault per crystallite (*6*). The fact that these nanocrystals are synthesized in the condensed phase adds an important degree of control to the sample preparation by allowing for chemical surface derivatization. This combination of properties makes this an ideal system for testing the effect of finite size on stable structures.

Bulk CdSe undergoes a phase transition

---

Materials Science Division, Lawrence Berkeley Laboratory, and Department of Chemistry, University of California, Berkeley, CA 94720, USA.